INTERNATIONAL ATOMIC ENERGY AGENCY
UNITED NATIONS EDUCATIONAL, SCIENTIFIC AND CULTURAL ORGANIZATION
INTERNATIONAL CENTRE FOR THEORETICAL PHYSICS
I.C.T.P., P.O. BOX 586, 34100 TRIESTE, ITALY, CABLE: CENTRATOM TRIESTE

H4.SMR/650-3

Workshop on Three-Dimensional Modelling of Seismic Waves Generation Propagation and their Inversion

30 November - 11 December 1992

Zoning of the Italian Territory in Terms of Expected Peak Ground Acceleration Derived from Complete Synthetic Seismograms

G. Costa (1), G.F. Panza (1,3), P. Suhadolc (1), F. Vaccari, (1,2) (*)

(1) Istituto di Geodesia e Geofisica, Università degli Studi di Trieste Trieste, Italy

(2) CNR, Gruppo Nazionale per la Difesa dei Terremoti

(3) International Centre for Theoretical Physics Trieste, Italy

(*) Authors listed in alphabetical order

ZONING OF THE ITALIAN TERRITORY IN TERMS OF EXPECTED PEAK GROUND ACCELERATION DERIVED FROM COMPLETE SYNTHETIC SEISMOGRAMS

Giovanni Costa[1], Giuliano Francesco Panza[1,3], Peter Suhadolc[1], Franco Vaccari[1,2] (*)

1 - Istituto di Geodesia e Geofisica, Università di Trieste

2 - CNR, Gruppo Nazionale per la Difesa dai Terremoti

3 - International Center for Theoretical Physics, Trieste

(*) - Authors listed in alphabetical order

ABSTRACT

An automatic procedure for the seismic zonation of a territory is presented. The results consist of deterministic computation of acceleration time series distributed on a regular grid over the territory. For the estimation of the accelerations, complete synthetic seismograms are computed by the modal summation technique. A first rough zonation can be accomplished by considering a map showing the distribution of peak ground acceleration. In this work the new procedure has been applied to the Italian territory. The structural and source models necessary to compute the synthetic signals have been fixed after an extensive bibliographic research. Seismogenic areas have been defined in the framework of the GNDT (Gruppo Nazionale per la Difesa dai Terremoti of the Consiglio Nazionale delle Ricerche, Rome) research activities dedicated to the definition of the kinematic model of Italy. Information on historical and recent seismicity has been taken from the most updated Italian earthquake catalogues. The estimated peak ground accelerations have been found to be compatible with available data, both in terms of intensity (historical earthquakes) and accelerations (recent earthquakes).

1. INTRODUCTION

The zonation of a territory in terms of seismic hazard is an essential preventive countermeasure in countries with high seismic risk, especially for densely populated areas. Maximum expected peak ground acceleration (PGA), at different frequencies, is a very important parameter considered by civil engineers when designing or reinforcing constructions.

We have developed a deterministic procedure which allows us to estimate PGA (routinely at frequencies as high as 10 Hz) starting from the available information on Earth structure parameters, seismic sources and the level of seismicity of the investigated area. Theoretical accelerations are computed by the modal summation technique (Panza, 1985; Florsch et al., 1991). The use of synthetic seismograms allows us to estimate in a realistic way the seismic hazard also in those areas for which scarce (or none) historical or instrumental information is available. It is also possible to simulate quite easily different kinds of source mechanisms, to consider different structural models and to compare the relative results in order to evaluate the influence of each parameter. To reduce the amount of computations, the seismic sources have been grouped in homogeneous seismogenic areas, and for each group the representative focal mechanism has been kept constant. The seismic moment associated with each source is determined from the analysis of the maximum magnitude observed in the epicentral area in the past.

One way of representing the result of the procedure is to analyse the synthetic seismograms and to map the distribution of PGA over the investigated territory. The synthetic signals used for the prediction of the accelerations can be conveniently used as input data for more detailed zoning, based on the 2D modelling of wave propagation (Fäh et al., 1990; Iodice et al., 1992). In this way, also the local soil effects can be taken into account.

The flow-chart of the procedure is shown in Figure 1. In the following text, references to the flow chart are written in *italics*.

2. DATA

To compute the synthetic seismograms, the structures containing the source and the receivers must be defined, as well as the source characteristics. On the basis of the geologic characteristics, the Italian territory has been divided into 16 *polygons* (Figure 2). A flat, layered *structural model* has been then associated with each polygon. The different layers are described by their thickness, density, P- and S-wave velocities and attenuation. The layering has been defined after an extensive bibliographic research, taking into account available DSS data (e.g. Bottari et al. 1982; Kern and Schenk, 1985; Italian Explosion Seismology Group and Institute of Geophysics ETH, 1981; Miller et al., 1982; Nicolas et al., 1990; Nicolich, 1981; Nicolich, 1989; Scarascia and Pellis, 1985; Schütte, 1978) and indirectly relevant data (e.g. Woollard, 1975).

The definition of the *seismic sources* has required the analysis of several data sets. To limit the spatial distribution of sources, we have used the 57 *seismogenic areas* (see Figure 3) defined by the GNDT (1992) on the basis of seismological data and seismotectonic observations (e.g. Patacca et al., 1992).

For the definition of the source mechanisms, 305 fault-plane solutions, distributed over the whole territory, have been grouped in a database (Suhadolc, 1990; Suhadolc et al., 1992). The computer file contains a standard definition of the *focal mechanisms*, both as a function of strike, dip and rake of the nodal planes and as a function of the direction of compressional, tensional and null axes.

For the analysis of seismicity, an *earthquake catalogue* (PFGING) has been prepared merging the data from the PFG (1985) catalogue, for the period 1000-1979, with the data from ING (1980-1991) bulletins, for the period 1980-1991. The original catalogues have been corrected for some obvious mistakes, like the presence of double or multiple events, time disorder and evident errors in the focal depths. Furthermore, only main shocks shallower than 50 km have been considered, removing aftershocks according to the algorithm suggested by Keilis-Borok et al. (1980).

We have considered only earthquakes that occurred within the PFG polygon (PFG, 1985). Therefore, the seismicity might be underestimated near political borders, and this could influence also the results (PGA distribution) in the regions close to these boundaries.

3. COMPUTATIONS

To derive the distribution of the maximum observed magnitude over the territory, the image of the seismicity given by the earthquake catalogue has been smoothed. At first, the area has been subdivided into 0.2° X 0.2° cells. Each cell has been assigned the magnitude value of the most energetic event that occurred within it. The smoothing obtained through this discretization, however, was not found to be satisfactory, since not each cell does contain a statistically meaningful number of events. Therefore, the maximum magnitude to be associated with each cell has been searched for also in the cell surroundings, through the application of a centred smoothing window. More details about the discretization and smoothing of seismicity are given in Appendix A.

For the definition of the seismic sources that are used to generate the synthetic seismograms, only the cells located within a seismogenic area are retained. The map shown in Figure 4 is the result of the application of this method to the PFGING earthquake catalogue.

A double-couple point source is then placed in the centre of each cell. The orientation of the double couple associated with each source is obtained from the database of the fault-plane solutions. For each seismogenic area, a representative focal mechanism is selected through an automatic procedure. As a first simple hypothesis, the tensor elements of these mechanisms have been defined as the arithmetic average of the tensor elements of the available mechanisms. This procedure appears to be reasonable when the mechanisms to average are not too different, and this condition has been checked for each seismogenic area.

Once the structures and the sources have been defined, *receivers* are placed on a grid (0.2° X 0.2°) covering the whole territory and synthetic seismograms are efficiently computed by

the modal summation technique (Panza, 1985; Florsch et al., 1991). In this first example, the synthetic signals are computed for an upper frequency content of 1 Hz, and the point-source approximation is still acceptable. This is fully justified by practical considerations, since for instance several-story buildings have a peak response in the frequency range below 1 Hz (e.g. Manos and Demosthenous, 1992). When shorter periods are considered, it will be no longer possible to neglect the finite dimensions of the faults and the rupturing process at the source.

To reduce the number of the computed seismograms, the source-receiver distance is kept below an upper threshold, which is taken to be a function of the magnitude associated with the source. The maximum source-receiver distance has been set equal to 25 km, 50km and 90 km, respectively for $M<6$, $6 \le M<7$ and $M \ge 7$. All seismograms have been computed for a constant hypocentral depth (10 km), but it is also possible to assign to each source an average depth determined from the analysis of catalogues of past seismicity. The reason to keep the hypocentral depth fixed and shallow is to be found in the large errors affecting the hypocentral depth estimates in the PFGING catalogue and in the fact that strong ground motion is mainly controlled by shallow sources (e.g. Vaccari et al., 1990).

P-SV (radial and vertical components) and *SH* (transverse component) *synthetic seismograms* are originally computed for a seismic moment of $1\ 10^{-7}$ N m. The amplitudes are then properly scaled according to the (smoothed) magnitude associated with the cell of the source. For the moment-magnitude relation, we have chosen the one given by Boore (1987). To obtain the values given in Table 1, which are valid for the frequency of 1 Hz, we have used the scaling law proposed by Gusev (1983). The idea of a constant magnitude within each seismogenic area (choosing the maximum available value) has been discarded because for the larger seismogenic areas it leads to an over-estimation of the seismicity.

At each receiver, the horizontal components are first rotated to a reference system common to the whole territory (North-South and East-West directions) and then the vector sum is computed. For the *significant parameters* representative of the strong ground motion we have, for the moment, focused our attention on the peak ground acceleration values (PGA). As we compute the complete

time series, we are not limited to this choice, and it is also possible to consider other parameters, like Arias (Arias, 1970) intensity or other integral quantities that can be of interest in seismic engineering. Since recordings of many different sources are associated to each receiver, but one single value is to be plotted on a map (Figure 5), only the maximum value of the analysed parameter is considered.

4 DISCUSSION AND CONCLUSIONS

The intensity-acceleration relation proposed by Boschi et al. (1969) has been used to compare the results of Figure 5 with the historical data, for which only macroseismic intensity estimates exist (see Table 2). We have checked that the computed PGA values are compatible with the above mentioned relation.

A more quantitative check has been made using the observed accelerograms recorded during the Irpinia earthquake on 23 November 1980. It is well known that the source rupturing process of that event is very complex (e.g. Bernard and Zollo, 1989), and the dimension of the source has been estimated to be of the order of several tens of km. Nevertheless, it looks as the signal recorded at the station of Sturno is mostly due to a single sub-event that occurred rather close to the station itself, while the energy contributions coming from other regions of the source seem irrelevant (Vaccari et al., 1990). We have low-pass filtered the NS accelerogram recorded at Sturno with a cut-off frequency at 1 Hz to compare it with one of the computed signals for the Irpinia region (Figure 6). The early phases and the PGA of the two time series are in very good agreement. The late part of the observed recording is more complicated and this is related to the complexity of the source, which has been neglected in the computation of the synthetic signal.

The definition of seismogenic structures of the Italian territory, given by GNDT (1982), is the final result of a fruitful cooperation between structural geologists and seismologists from all over Italy. In developing the project, several proposals have been made and some provisional hypothesis have been considered. Taking advantage of those existing alternatives, it has been

possible to test the stability of our results, namely the PGA distribution, versus the distribution of seismogenic structures. Model A is one intermediate result of the GNDT project, as it does not include the Alpine Arc (Figure 7) and can be compared with the more recent, presently accepted, model of Figure 3, which was used to compute the PGA distribution shown in Figure 5. In the common regions, some relevant differences can be evidenced in the Lazio and Toscana regions, as well as in the Gargano peninsula. Furthermore, in the more recent model, the Calabrian Arc is characterised by a much more simplified zonation. The smoothed magnitude associated with the seismogenic zones of Model A are given in Figure 8. Figure 9 shows the PGA distribution obtained using Model A and should be compared with Figure 5. It can be noticed that in the common areas the regions where maximum accelerations are expected to occur are almost the same, and also the PGA values do not differ too much. Relevant discrepancies, between 0.1 and 0.2g, can only be found in relation to the Calabrian Arc (see Figure 10) where, due to the larger spatial extension of seismogenic areas, Model A implies PGA values also in the class 0.40-0.50g.

This comparison shows one important advantage of the procedure, namely the possibility of easily testing the influence of any parameter that is used as input data. An important stability test will be performed as soon as the revised earthquake catalogue by GNDT will be available. Stability tests are currently being performed analysing the catalogues in different periods of time.

REFERENCES

Arias, A., 1970. A measure of earthquake intensity. In: R. Hansen (Editor), Seismic design for nuclear power plants. Cambridge, Massachussets.

Bernard, P. and Zollo, A., 1989. The Irpinia (Italy) 1980 earthquake: detailed analysis of a complex normal faulting. J. Geophys. Res., 94:1631-1647.

Boore, D.M., 1987. The prediction of strong ground motion. In: M.Ö. Erdik and M.N. Toksöz (Editors), Strong ground motion seismology, D. Reidel Publishing Company, Dordrecht, Holland, pp. 109-141.

Boschi, E., Caputo, M. and Panza, G.F., 1969. Stability of Seismic Activity in Italy With Special Reference to Garfagnana, Mugello and Forlivese, Rapporto CNEN RT/ING(69)24.

Bottari, A., Caccamo, D., Carapezza, E., Cosentino, M., Cosentino, P., Federico, B., Fradella, P., Hoang Trong, P., Lo Giudice, E., Lombardo, G., Neri, G. and Patanè, G., 1982. Crustal regional travel times of P and S waves in Sicily. CNR, Roma. Atti 2° Convegno GNGTS, pp. 605-614.

Fäh, D., Suhadolc, P. and Panza, G.F., 1990. Estimation of Strong Ground Motion in Laterally Heterogenenous Media: Modal Summation - Finite Differences. Proc. 9-th European Conference of Earthquake Engineering, Sept. 11-16, 1990, Moscow, USSR, 4A:100-109.

Florsch, N., Fäh, D., Suhadolc, P. and Panza, G.F., 1991. Complete synthetic seismograms for high-frequency multimode Love waves, PAGEOPH, 136:529-560.

GNDT, 1992. Convegno Nazionale sul Modello Sismotettonico d'Italia. Milano, 25-26 May.

Gusev, A.A., 1983. Descriptive statistical model of earthquake source radiation and its application to an estimation of short period strong motion. Geophys. J.R. Astron. Soc., 74:787-800.

ING, 1980-1991. Istituto Nazionale di Geofisica. Seismological reports. ING, Roma.

Iodice, C., Fäh, D., Suhadolc, P. and Panza, G.F., 1992. Un metodo generale per la zonazione sismica rapida ed accurata di grandi metropoli: applicazione alla città di Roma. Memorie dell'Accademia Nazionale dei Lincei. 3:000-000.

Italian Explosion Seismology Group and Institute of Geophysics, ETH, Zürich, 1981. Crust and upper mantle structures in the Southern Alps from deep seismic sounding profiles (1977, 1978) and surface waves dispersion analysis. Boll. di Geof. teor. ed appl., 23:297-330.

Keilis-Borok, V.I., Knopoff, L., Rotwain, I.M. and Sidorenko, T.M., 1980. Bursts of seismicity as long-term precursors of strong earthquakes. J. Geophys. Res., 85:803-812.

Kern, H. and Schenk, V., 1985. Elastic wave velocities from a lower crustal section in Southern Calabria (Italy). Phys. Earth Planet. Inter., 40:147-160.

Manos, G.C. and Demosthenous, M., 1992. Design of R.C. structures according to the Greek Seismic Code Provisions. Bull. of IISEE, 26:559-578.

Miller, H., Müller, St. and Perrier, G., 1982. Structure and dynamics of the Alps: a geophysical inventory. In: H. Berkhemer and U. Hsü (Editors) Alpine-Mediterranean Geodynamics, Geophys. Ser. A.G.U., 7:175-203.

Nicolich, R., 1981. Il profilo Latina-Pescara e le registrazioni mediante OBS nel Mar Tirreno. CNR, Roma. Atti del 1° Convegno GNGTS, pp. 621-634.

Nicolich, R., 1989. Crustal structures from seismic studies in the frame of the European Geotraverse (Southern Segment) and CROP projects. Atti Convegni Lincei, 80:41-61.

Nicolas, A., Polino, R., Hirn, A., Nicolich, R. and ECORS-CROP Working Group, 1990. ECORS-CROP traverse and deep structures in the Western Alps. In: Deep Structure of the Alps special issue, Soc. Geol. de France, Italie et Suisse.

Panza, G. F., 1985. Synthetic seismograms: The Rayleigh waves modal summation. J. Geophysics, 58:125-145.

Panza, G. F., Prozorov, A. and Suhadolc, P., 1990. Is there a correlation between lithosphere structure and statistical properties of seismicity? In: R. Cassinis and G. F. Panza (Editors), The structure of the Alpine - Mediterranean area: contribution of geophysical methods, Terra nova, 2:585-595.

Patacca, E., Sartori, R. and Scandone, P., 1992. Tyrrhenian basin and Apenninic arcs: kinematic relations since late Tortonian times. Mem. Soc. Geol. It., in press.

PFG 1985. D. Postpischl (Editor), Catalogo dei terremoti italiani dall'anno 1000 al 1980 (). CNR-Progetto Finalizzato Geodinamica.

Scarascia, S. and G. Pellis 1985. Crustal structure of the Northern Apennine. Part A - The upper crust. In: D.A. Galson and St. Müller (Eds.). Proceedings of the Second Workshop on the European Geotraverse (EGT) Project. The Southern Segment. European Science Fundation, Strasbourg, 137-142.

Schütte, K.G. 1978. Crustal structure of Southern Italy. In: H. Closs, D. Roeder and K. Schmidt (Eds.) Alps, Apennines and Hellenides, IUGG, 38, 374-388.

Suhadolc, P. 1990. Fault-plane solutions and seismicity around the EGT southern segment. In: R. Freeman and St. Müller (Eds.), Sixth EGT Workshop: Data Compilations and Synoptic Interpretation, European Science Foundation, Strasbourg, 371-382.

Suhadolc, P., Panza, G.F., Marson, I., Costa, G. and F. Vaccari 1992. Analisi della sismicità e meccanismi focali nell'area italiana. *Atti del Convegno del Gruppo Nazionale per la Difesa dai Terremoti*, Pisa 1990, 1, 157-168.

Vaccari, F., Suhadolc, P. and G.F. Panza 1990. Irpinia, Italy, 1980 earthquake: waveform modelling of strong motion data, *Geophys. J. Int.*, 101, 631-647.

Woollard, G.P. 1975. Regional changes in gravity and their relation to crustal parameters. *Bur. Grav. Int. Bull. d'Inf.*, 36, 106-110.

APPENDIX A

Discretization and smoothing of seismicity.

The first problem to tackle in the definition of seismic sources is the handling of seismicity data. What is needed by the procedure described in this paper and will be used in the computation of synthetic seismograms is a distribution over the territory of the maximum magnitude. Data available from earthquake catalogues are, on the contrary, discrete and punctual. Furthermore, a 2-dimensional distribution requires a large amount of samples to be well determined, but earthquake catalogues are both incomplete and affected by errors, so a smoothed distribution is preferable (Panza et al., 1990). A smooth distribution can be misleading in the fact that it assignes some values also to areas where data are absent. To avoid this drawback, we have decided to represent seismicity by cells. The size of the cells can be related with errors in the location of earthquakes. On the basis of experience (Suhadolc, 1990) the dimensions of 0.2° X 0.2° have been chosen, even if for historical earthquakes such a resolution could be considered optimistic.

The smoothing procedure is shown in Figure 11. At first, the punctual distribution of epicentres given in Figure 11a is discretised into cells (Figure 11b) and the maximum magnitude of the events pertinent to each cell is retained. In case the earthquake catalogue contains different estimates of the magnitude (e.g. magnitude computed from body waves, from surface waves, from macroseismic intensity), the maximum between them is considered. It is then convenient to represent the data graphically, where symbols are associated with magnitude ranges (Figure 11c).

In most cases, the smoothing obtained by just considering cells is not enough, since from a statistical point of view single cells do not contain a meaningful number of events. A centered smoothing window is then considered. Earthquake magnitudes are analysed not only in the central cell, but also in neighboring ones. The maximum value of magnitude found in the window is assigned to the central cell only if the cell itself contains a minimum number of earthquakes. For this purpose, several thresholds have been tested (one to four earthquakes): the increase in the threshold is related to a more stable representation of seismicity, since sporadic events, that could

be the result of mislocations or singularities of the seismic regime, are eliminated. We have noticed that only areas with very low seismicity, not included in the seismogenic areas shown in Figure 3, are sensible to modifications of the threshold in the range 1 to 3. Therefore, taking into consideration only the seismogenic areas, stability is already ensured if the lower threshold (one earthquake) is selected.

Three possible smoothing windows are shown in Figure 11d. Their "radius" is expressed in terms of number of cells n. In the example, the values n=1, n=2 and n=3 are considered. By applying those windows to the distribution of Figure 11c, the results of Figure 11e are obtained. At a first glance, it appears that the distribution of maximum magnitude given by the window with n=3 is quite exaggerated with respect to the starting data of Figure 11c, but its intersection with an hypothetic seismogenic area (shown in Figure 12a) gives quite reasonable results (Figure 12b).

The smoothing algorithm has been applied to the catalogue of main shocks for the Italian territory. Windows of radius n=0 (which corresponds to considering just the central cell), n=1, n=2 and n=3 have been used, obtaining the results shown in Figure 13a-d respectively. The intersection of the map of Figure 13d with the seismogenic areas of Figure 3, defined by GNDT (1992), is already shown in Figure 4. The radius n=3 has been selected since a good degree of homogeneity in the distribution of magnitude seems appropriate within each seismogenic area. This condition is not verified if the smoothing is not applied (see Figure 14).

Table 1

M	$M_{0\,(1Hz)}$ (N m)
8.00≥ >7.75	$4.00\ 10^{18}$
7.75≥ >7.50	$2.50\ 10^{18}$
7.50≥ >7.25	$1.60\ 10^{18}$
7.25≥ >7.00	$1.25\ 10^{18}$
7.00≥ >6.75	$5.00\ 10^{17}$
6.75≥ >6.50	$3.15\ 10^{17}$
6.50≥ >6.00	$1.60\ 10^{17}$
6.00≥ >5.50	$4.00\ 10^{16}$
5.50≥ >5.00	$1.40\ 10^{16}$
5.00≥	$4.00\ 10^{15}$

Table 2

Intensity	Acceleration (Boschi et al., 1969)	
	cm/s^2	g
XII	492.5	0.50
XI	370.9	0.38
X	284.4	0.29
IX	222.1	0.23
VIII	176.5	0.18
VII	142.9	0.15
VI	117.7	0.12
V	98.7	0.10
IV	84.3	0.09

FIGURE CAPTIONS

Figure 1. a) Flow-chart of the procedure; b) detail relative to the definition of seismic sources.

Figure 2. Regional polygons associated with different structural models. The grid of dots represent the location of the receivers where synthetic seismograms have been computed.

Figure 3. Seismogenic zones defined by GNDT (1992). C: compressional areas; E: extensional areas ; F: areas of fracture in foreland zones; T: transition areas; TP: areas of transpression; U: uncertain areas; V: volcanic areas.

Figure 4. Smoothed magnitude distribution for the cells belonging to the seismogenic zones shown in Figure 3.

Figure 5. Estimated distribution of horizontal peak ground acceleration.

Figure 6. Comparison between NS acceleration recorded at the station of Sturno during the Irpinia earthquake of 23 November 1980 (above) and one synthetic signal computed for that area (below) on the basis of the procedure described in this work. Accelerations have been low-pass filtered with a cut-off frequency of 1 Hz.

Figure 7. Seismogenic zones given by GNDT as a preliminary result in the seismogenic zonation of the Italian territory. This model, that we refer to as Model A, must be compared with the one shown in Figure 3. C: compressional areas; E: extensional areas; F: areas of fracture in foreland zones; T: transition areas.

Figure 8. Smoothed magnitude distribution for the cells belonging to the seismogenic zones shown in Figure 7.

Figure 9. Estimated distribution of the horizontal peak ground acceleration obtained using the seismogenic zones of Figure 7. For a stability test it should be compared with Figure 5.

Figure 10. Map of the relevant discrepancies between the PGA values shown in Figure 5 and Figure 9.

Figure 11. Discretization and smoothing of seismicity. a) Distribution of epicentres; b) definition of cells and choice of maximum magnitude; c) graphic representation of b); d) smoothing windows of radius n=1, n=2, n=3; e) smoothed distribution of magnitude.

Figure 12. a) Hypothetical seismogenic zone and b) its intersection with the example data of Figure 11e.

Figure 13. Magnitude distribution after the application of discretization and smoothing to the seismicity data given in catalogue PFGING after aftershock removal. Radius of smoothing window: a) n=0; b) n=1; c) n=2; d) n=3.

Figure 14. Intersection between the seismogenic zones of Figure 3 and the seismicity image of Figure 13a.

Fig. 1a

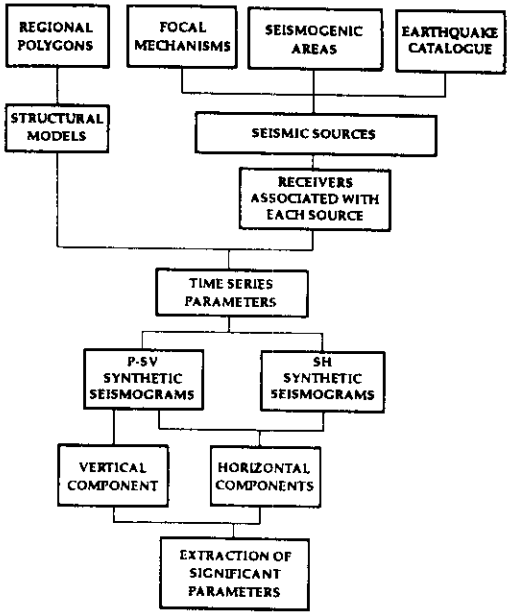
REGIONAL POLYGONS
FOCAL MECHANISMS
SEISMOGENIC AREAS
EARTHQUAKE CATALOGUE
STRUCTURAL MODELS
SEISMIC SOURCES
RECEIVERS ASSOCIATED WITH EACH SOURCE
TIME SERIES PARAMETERS
P-SV SYNTHETIC SEISMOGRAMS
SH SYNTHETIC SEISMOGRAMS
VERTICAL COMPONENT
HORIZONTAL COMPONENTS
EXTRACTION OF SIGNIFICANT PARAMETERS

Fig. 1b

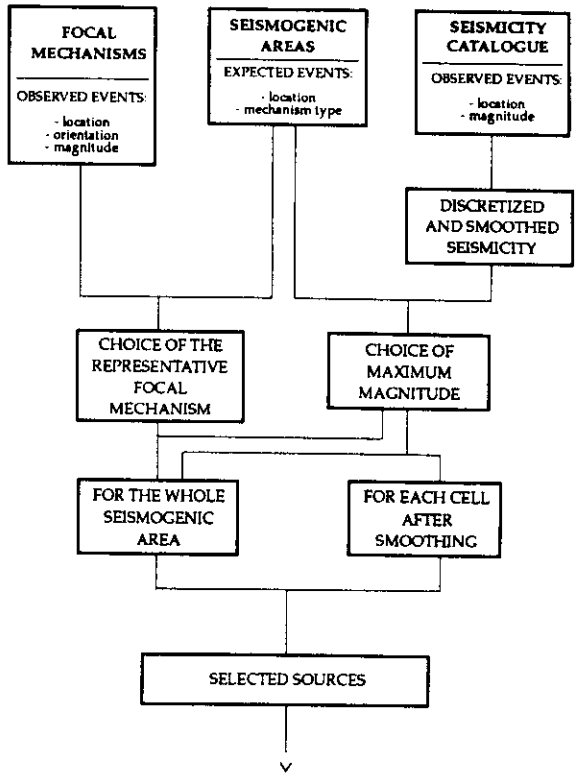
FOCAL MECHANISMS
OBSERVED EVENTS:
- location
- orientation
- magnitude
SEISMOGENIC AREAS
EXPECTED EVENTS:
- location
- mechanism type
SEISMICITY CATALOGUE
OBSERVED EVENTS:
- location
- magnitude
DISCRETIZED AND SMOOTHED SEISMICITY
CHOICE OF THE REPRESENTATIVE FOCAL MECHANISM
CHOICE OF MAXIMUM MAGNITUDE
FOR THE WHOLE SEISMOGENIC AREA
FOR EACH CELL AFTER SMOOTHING
SELECTED SOURCES

figure 2

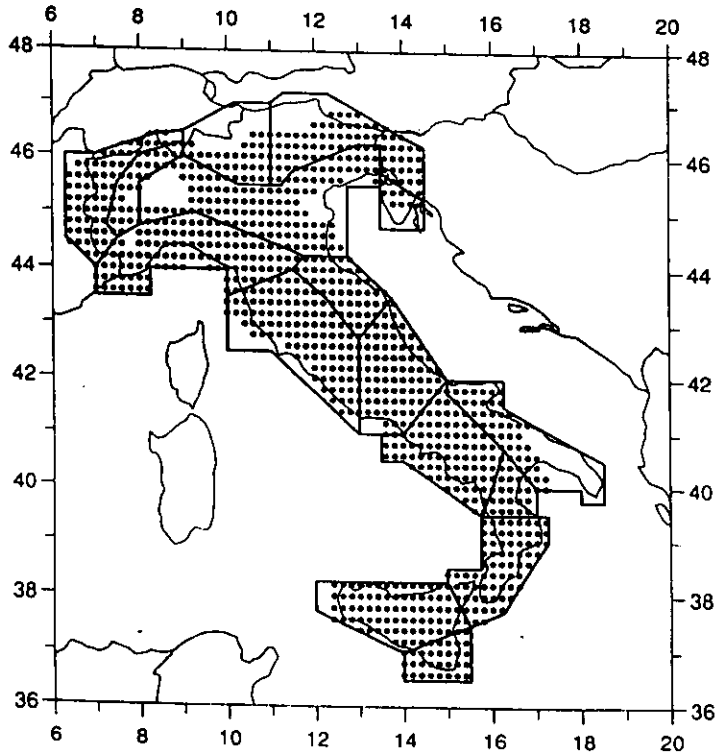

fig. 3

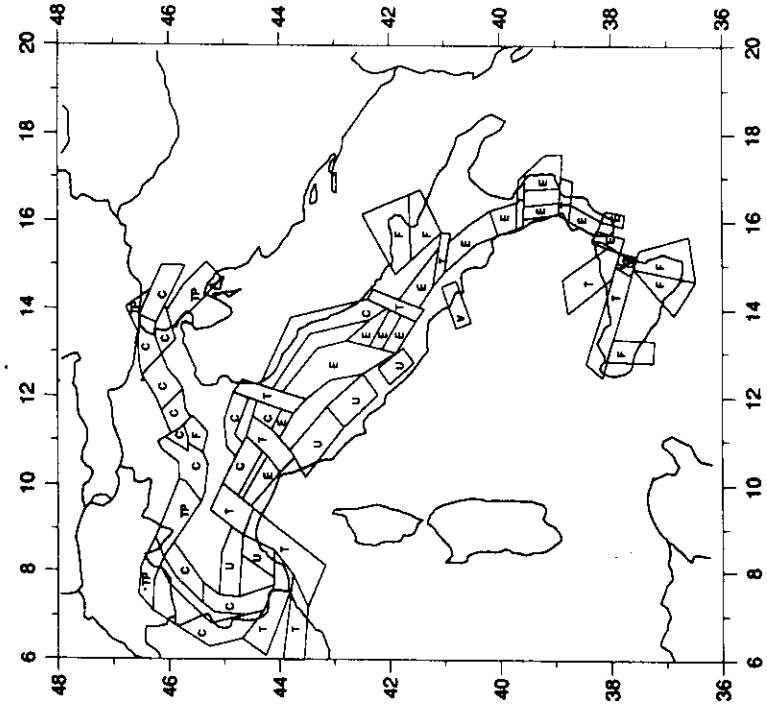

n = 3

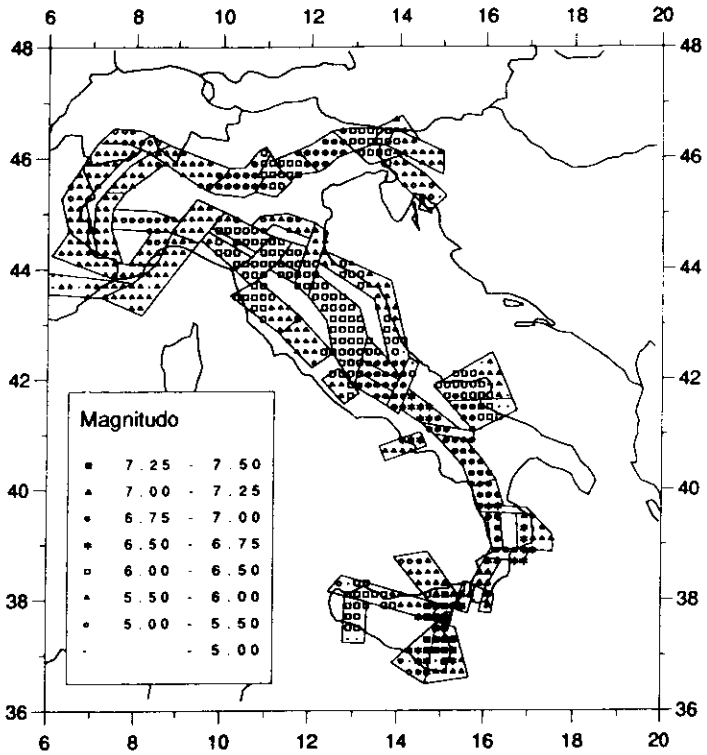
Magnitudo
7.25 - 7.50
7.00 - 7.25
6.75 - 7.00
6.50 - 6.75
6.00 - 6.50
5.50 - 6.00
5.00 - 5.50
- 5.00

C

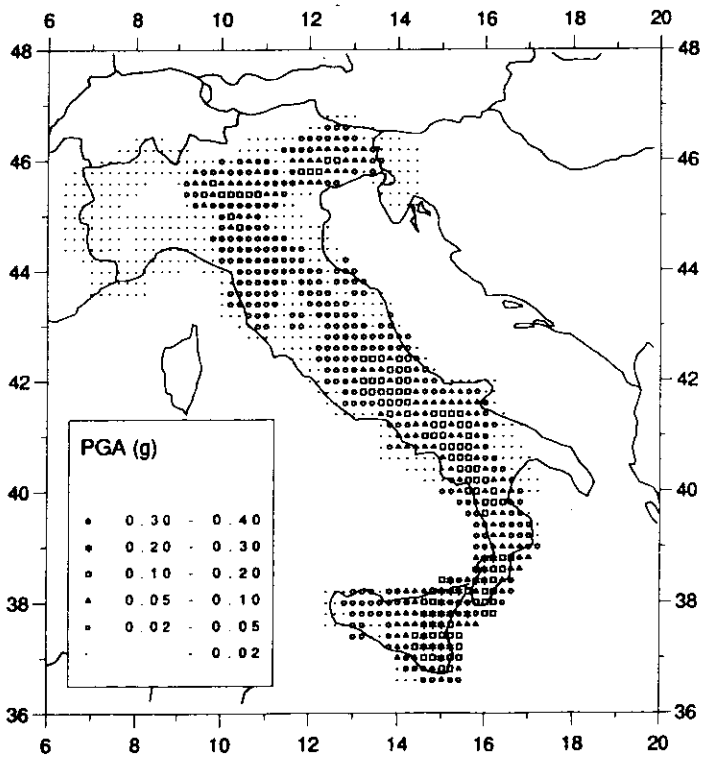
PGA (g)
0.30 - 0.40
0.20 - 0.30
0.10 - 0.20
0.05 - 0.10
0.02 - 0.05
- 0.02

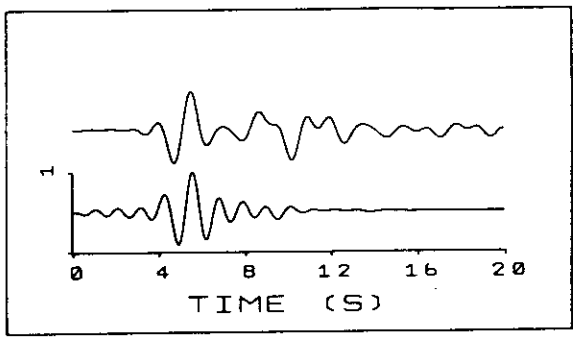

figure 6

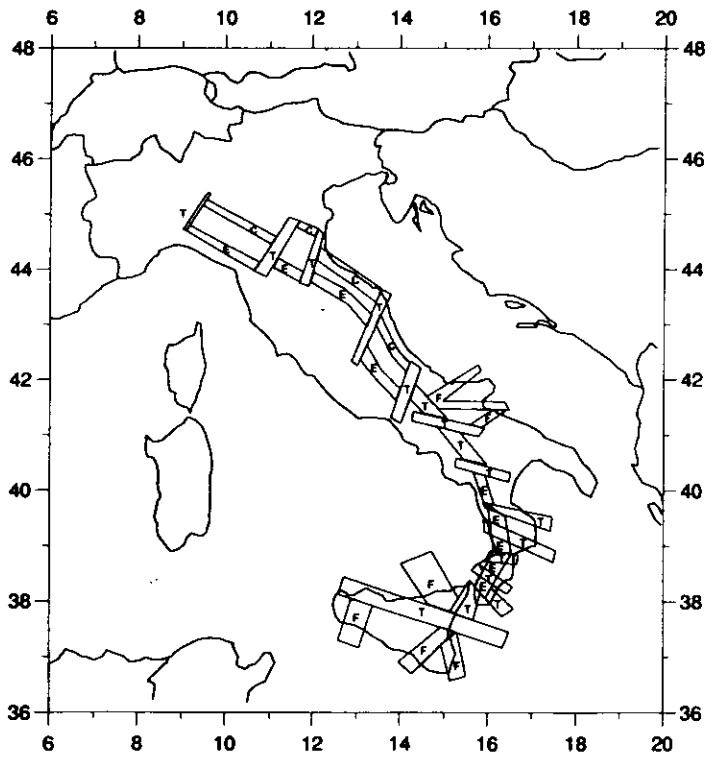

n = 3

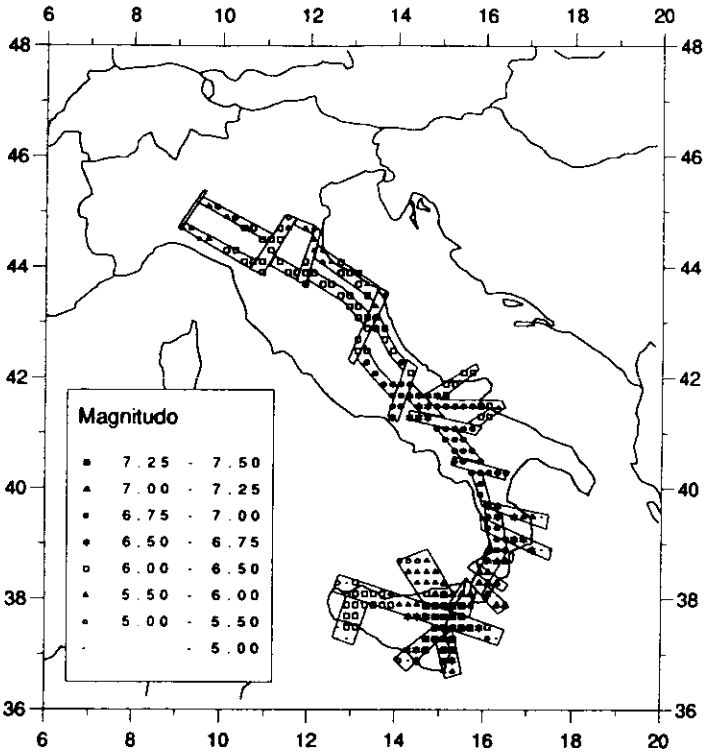
Magnitudo
7.25 - 7.50
7.00 - 7.25
6.75 - 7.00
6.50 - 6.75
6.00 - 6.50
5.50 - 6.00
5.00 - 5.50
- 5.00

A

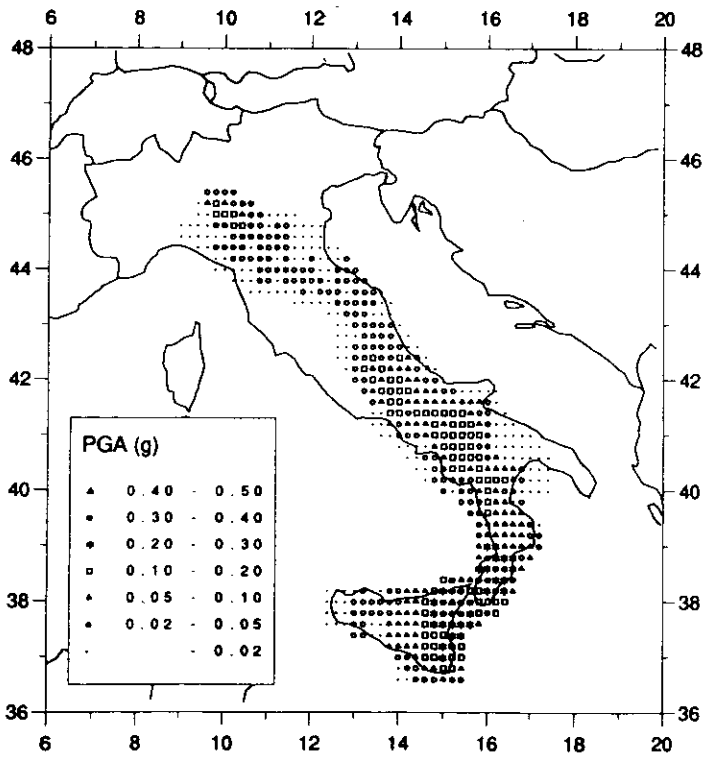
PGA (g)
0.40 - 0.50
0.30 - 0.40
0.20 - 0.30
0.10 - 0.20
0.05 - 0.10
0.02 - 0.05
- 0.02

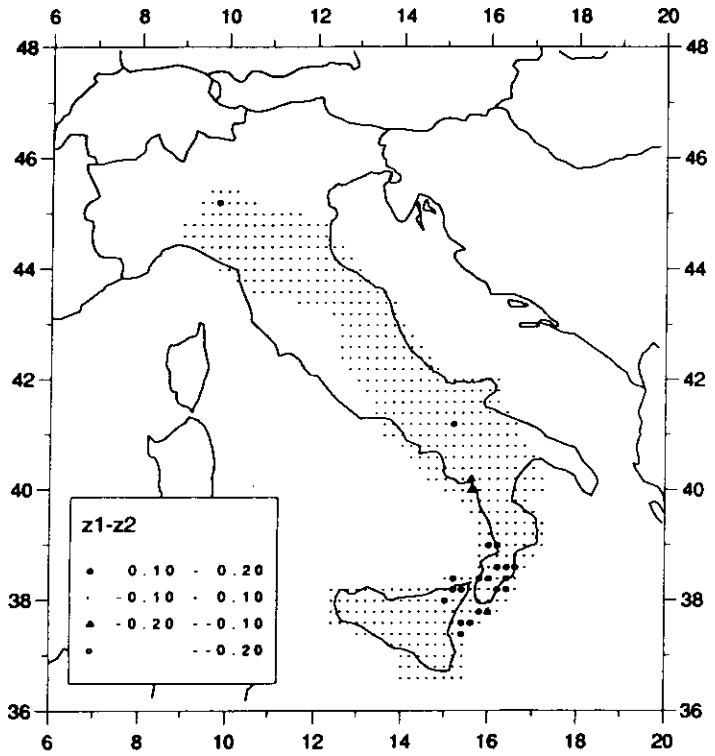

Fig. 10

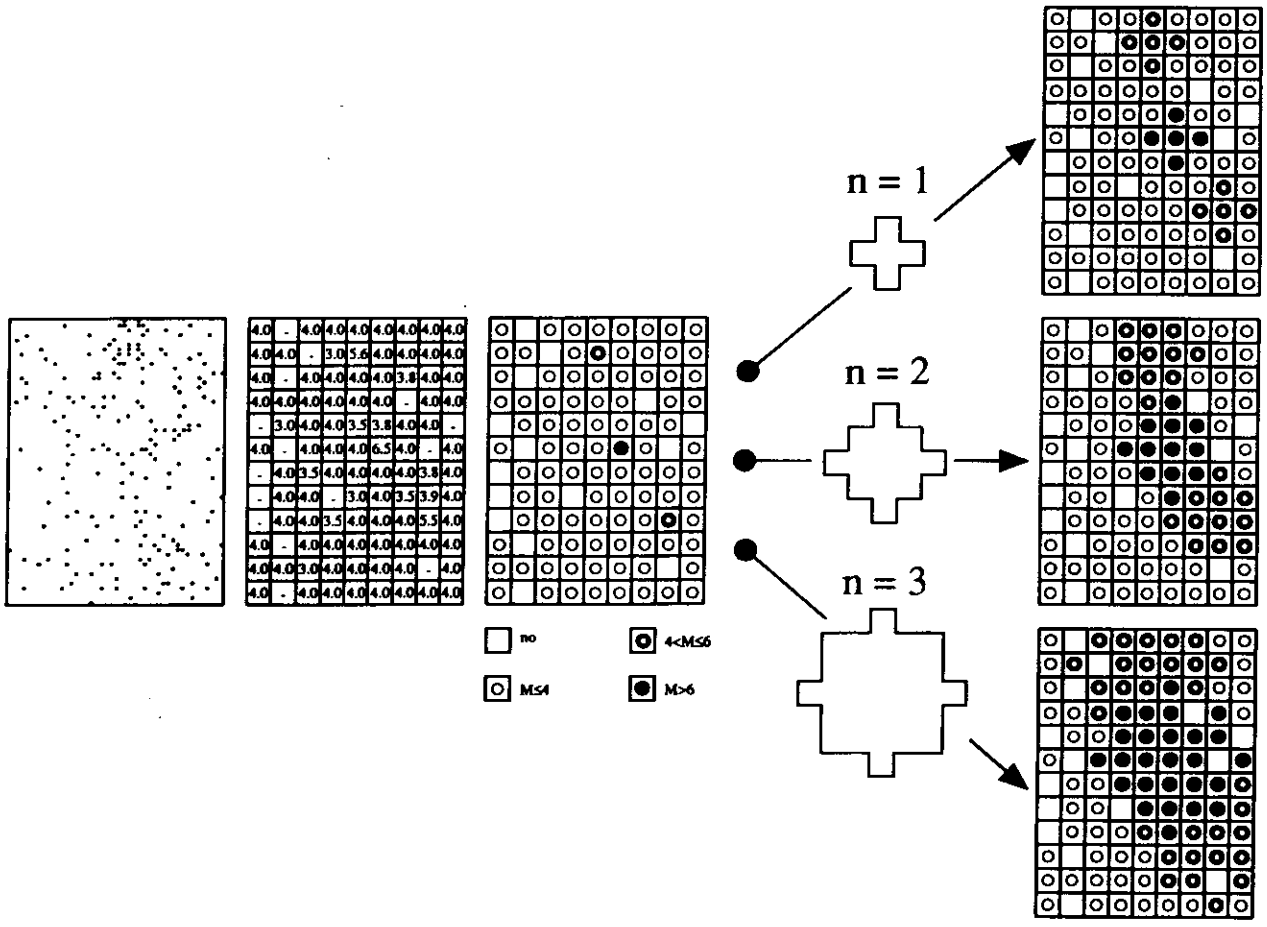

Fig. 11

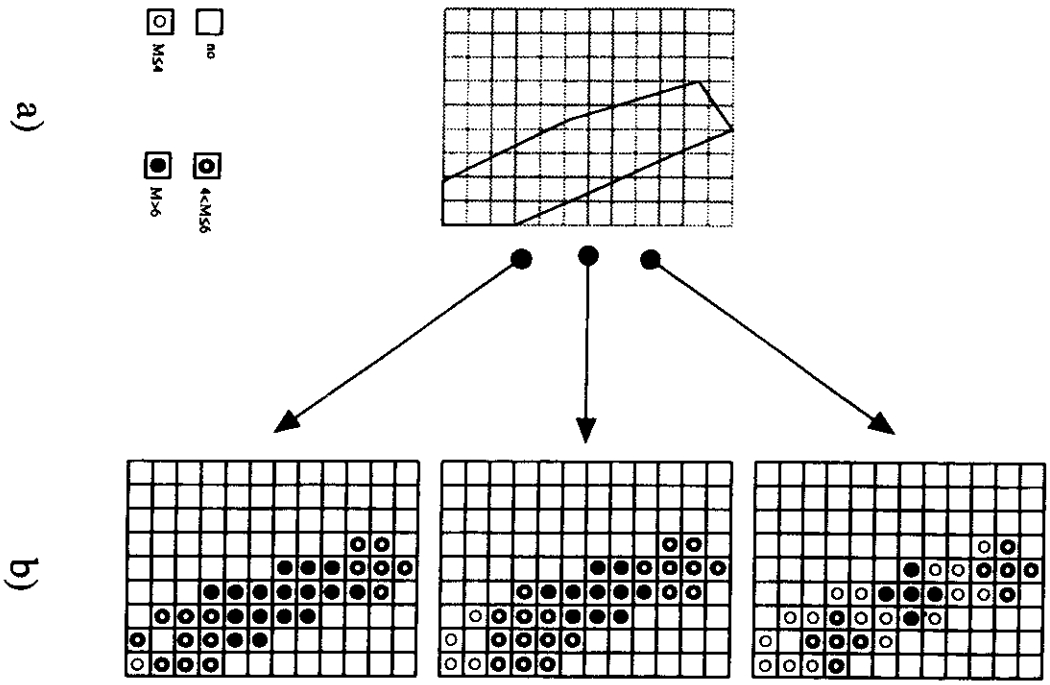
a)
b)
M≤4
no
M>6
4<M≤6

n = 0

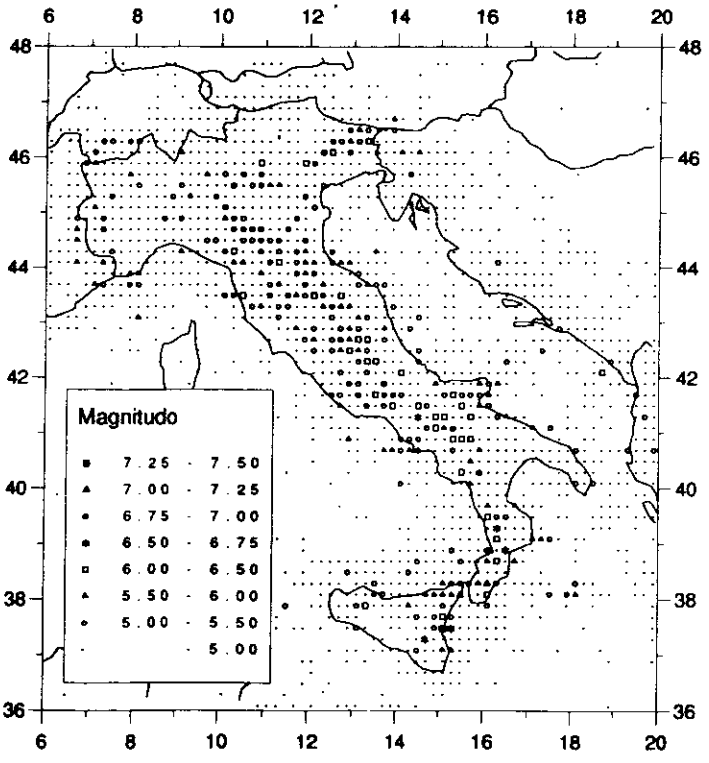
Magnitudo
7.25 - 7.50
7.00 - 7.25
6.75 - 7.00
6.50 - 6.75
6.00 - 6.50
5.50 - 6.00
5.00 - 5.50
- 5.00

n = 1

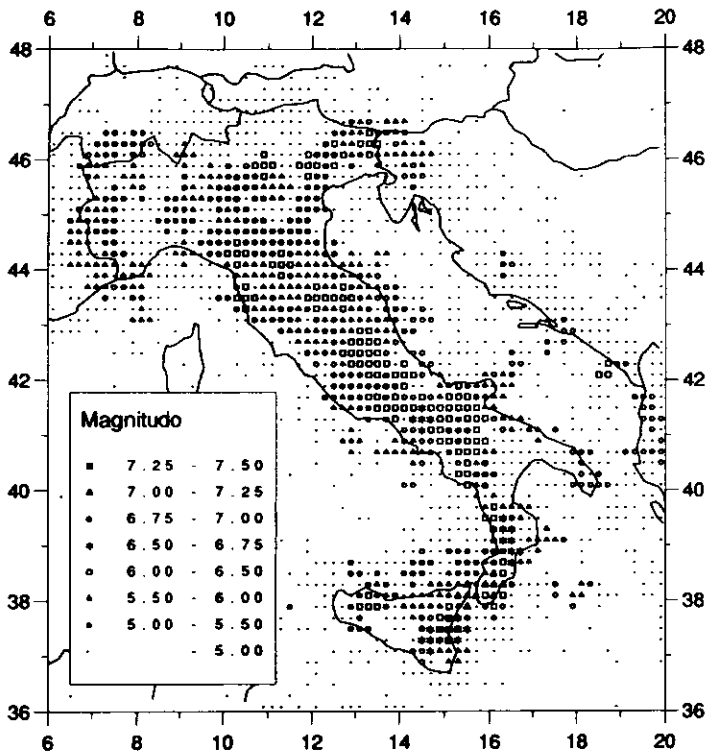

fig. 13b

n = 2

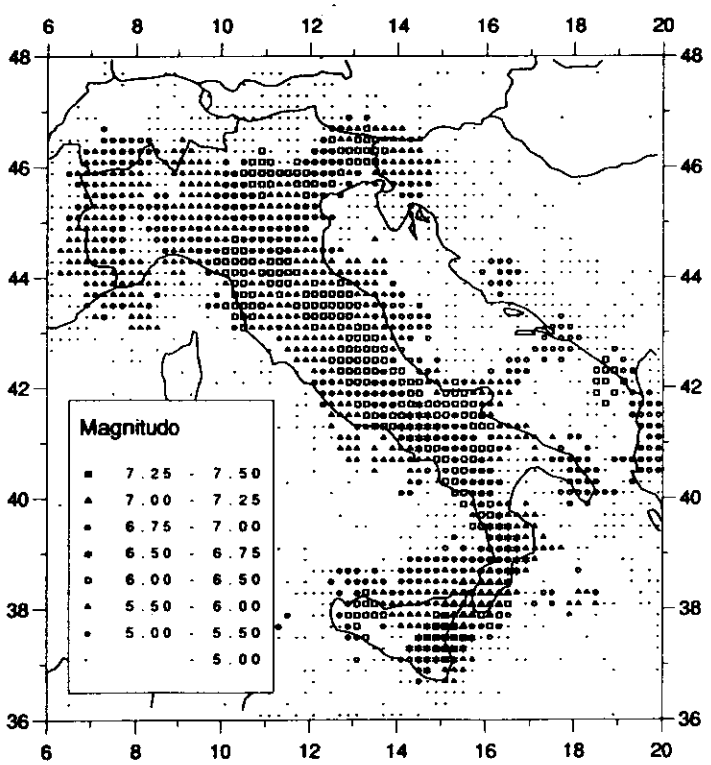

fig. 13c

n = 3

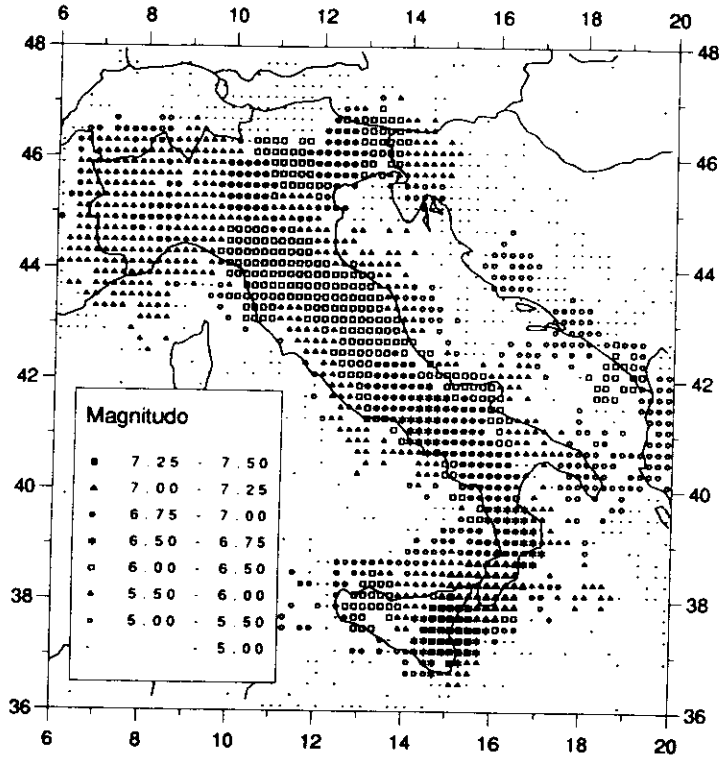

Fig 13a

n = 0

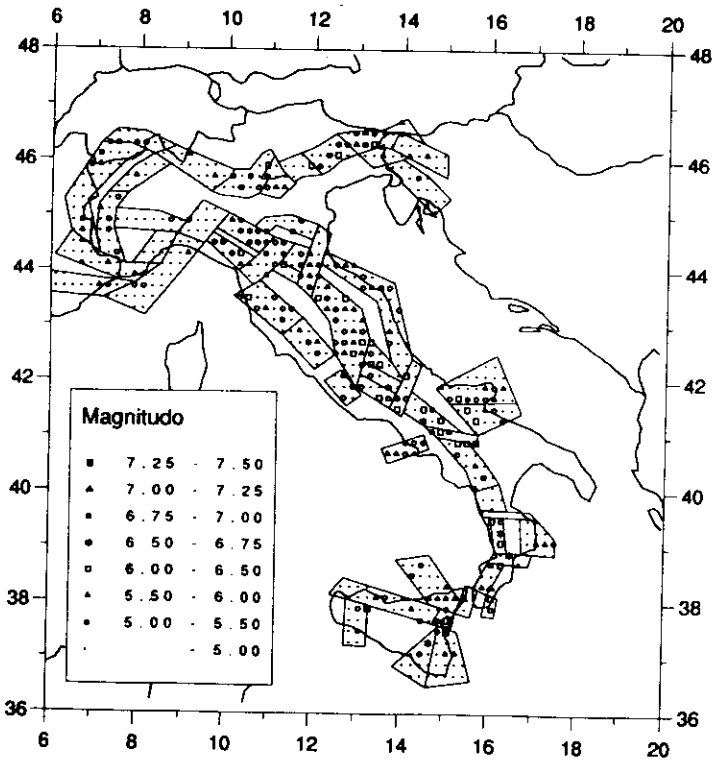

Fig 14